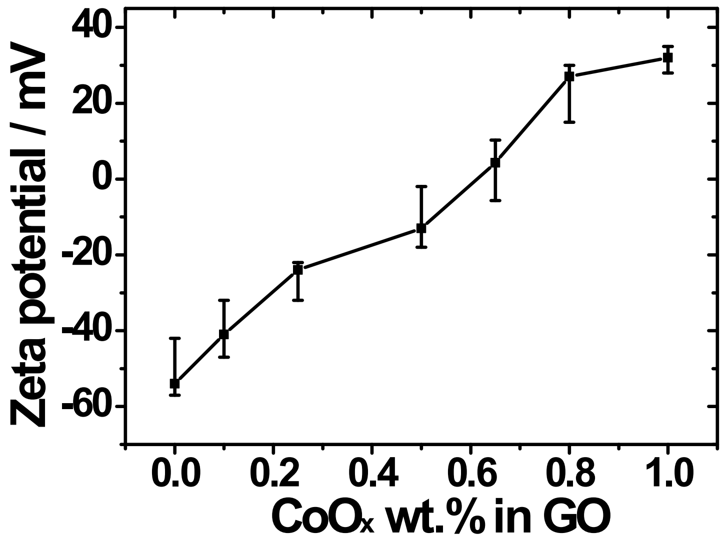

Fig. S1 Zeta potential measurement for the nanocomposites of CoO_x and GO at different ratios.

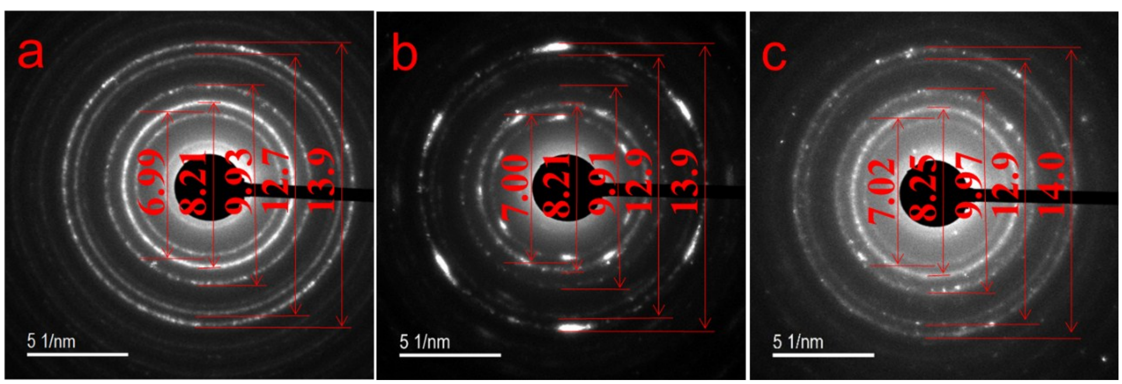

Fig. S2 Diffraction patterns for (a) Co_3O_4 NP/rGO, (b) Co_3O_4 NR/rGO and (c) Co_3O_4 NP/NGO samples. The values indicate the diameters for the ring that corresponds to 2/d-spacing.

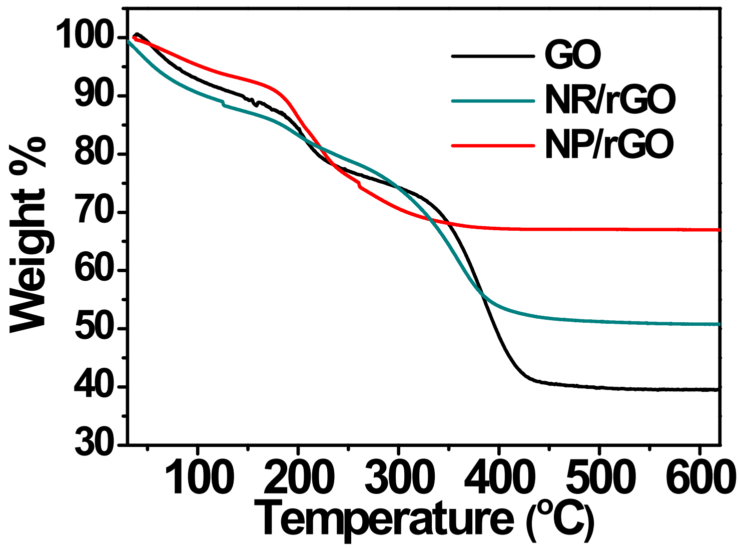

Fig. S3 TGA results for the HNCs of pure GO, NR/rGO and NP/rGO.

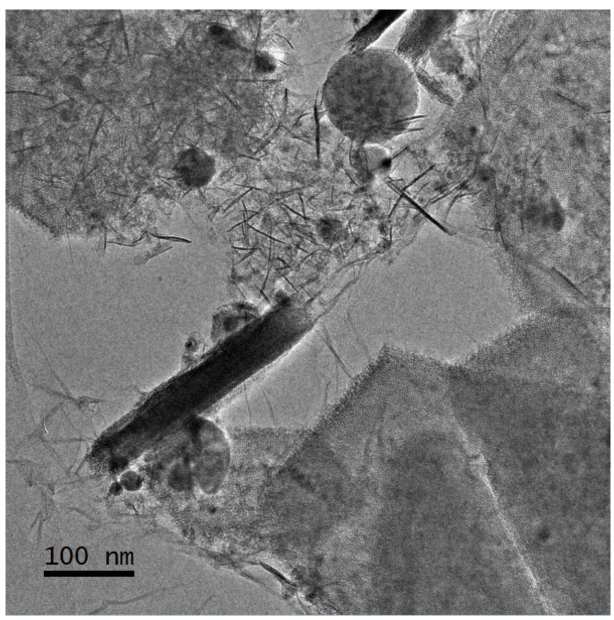

Fig. S4 TEM image of NR/rGO before heating

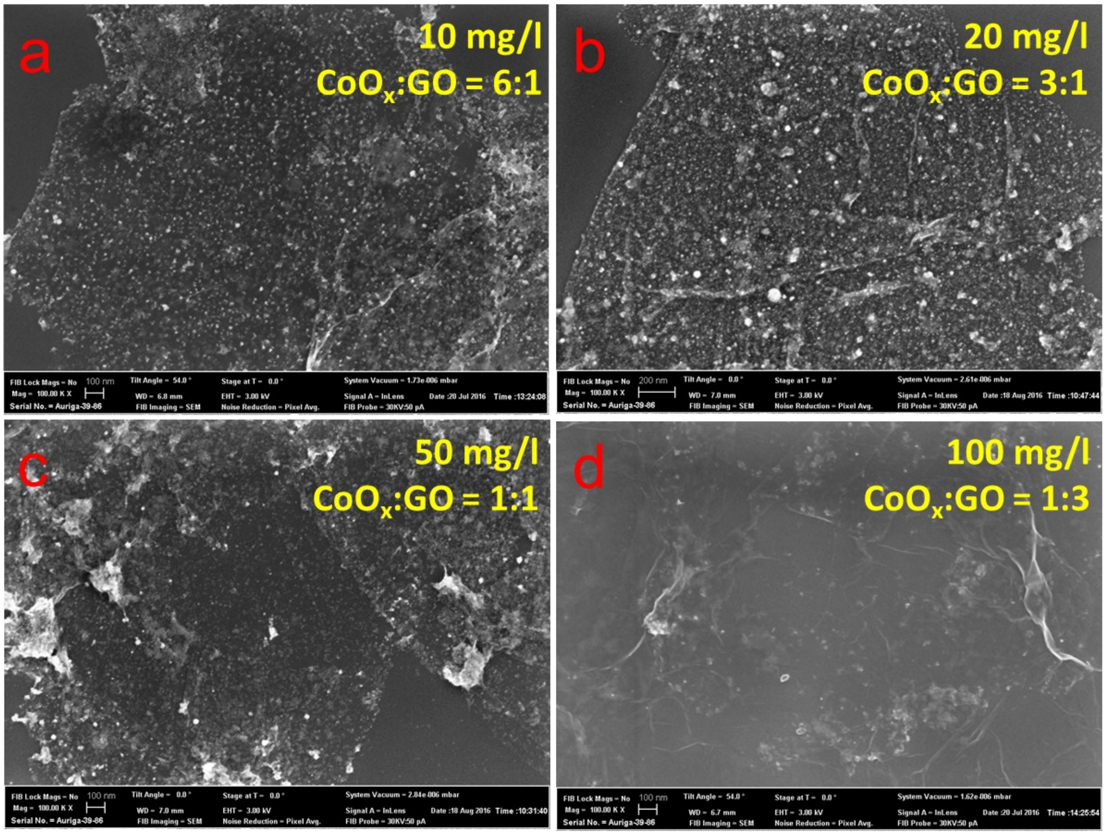

Fig. S5 SEM images for the nanocomposites of CoO_x and GO at different ratios.

Laser-induced breakdown spectroscopy (LIBS) has been used for quantitative compositional analysis of NP/NGO and NP/rGO. Specifically, the weight ratios of cobalt oxides to carbon Co_3O_4:C were obtained using an internal calibration technique [1-3]. Using the previous study set-up [3], the atomic emissions from cobalt and carbon were collected the quantitative analysis. Based on the relative lines strength, and transition probabilities, C I (247.86nm) and Co I (345.35nm) were chosen from the NIST Atomic Energy Levels Data Center [4] (Table S2). Fig. S6 shows the resolved emissions from NGO at 3.5us and 4us respectively. Based on the internal calibration method [1-3], the elemental ratio for NP/NGO is calculated as:

$$R = \frac{[\mathrm{Co}]}{[\mathrm{C}]} = \frac{[\mathrm{N}_{\mathrm{i}}^{Co\,\mathrm{I}(345.35\mathrm{nm})} / \mathrm{N}_{\mathrm{i}}^{Co\,\mathrm{I}}]_{@\mathrm{GD}=4\mu\mathrm{s}}}{[\mathrm{N}_{\mathrm{i}}^{\mathrm{C\,I}(247.86\mathrm{nm})} / \mathrm{N}_{\mathrm{i}}^{Co\,\mathrm{I}}]_{@\mathrm{GD}=3.5\mu\mathrm{s}}}$$

Where N_i^X represents the population density of species X. Therefore, the Co_3O_4:C weight ratio for NP/NGO and NP/rGO is estimated to be 3:1. Similarly, the Co_3O_4/C for NR/rGO is obtained as 3:2.

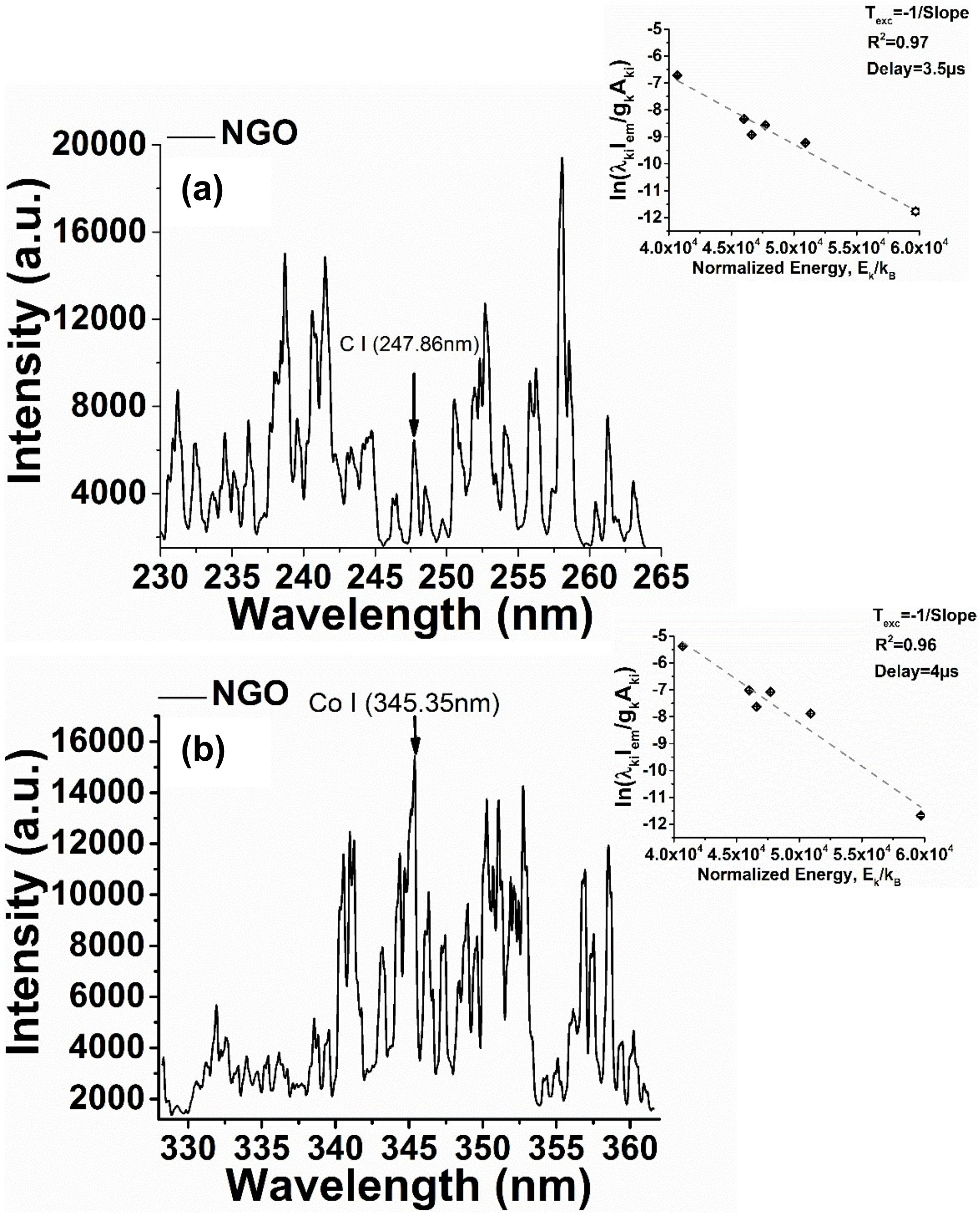

Fig. S6 Spectral emission signature for NP/NGO at (a) C I (247.86 nm), and (b) Co I (345.35 nm) lines at the respective gate delays of 3.5 μs, and 4 μs (Spectral details provided in Table S2). Inset shows the linear Boltzmann plots generated from Co I lines listed in Table S3, and used for T_{exc} calculations at the respective gate delays of 3.5 μs and 4 μs.

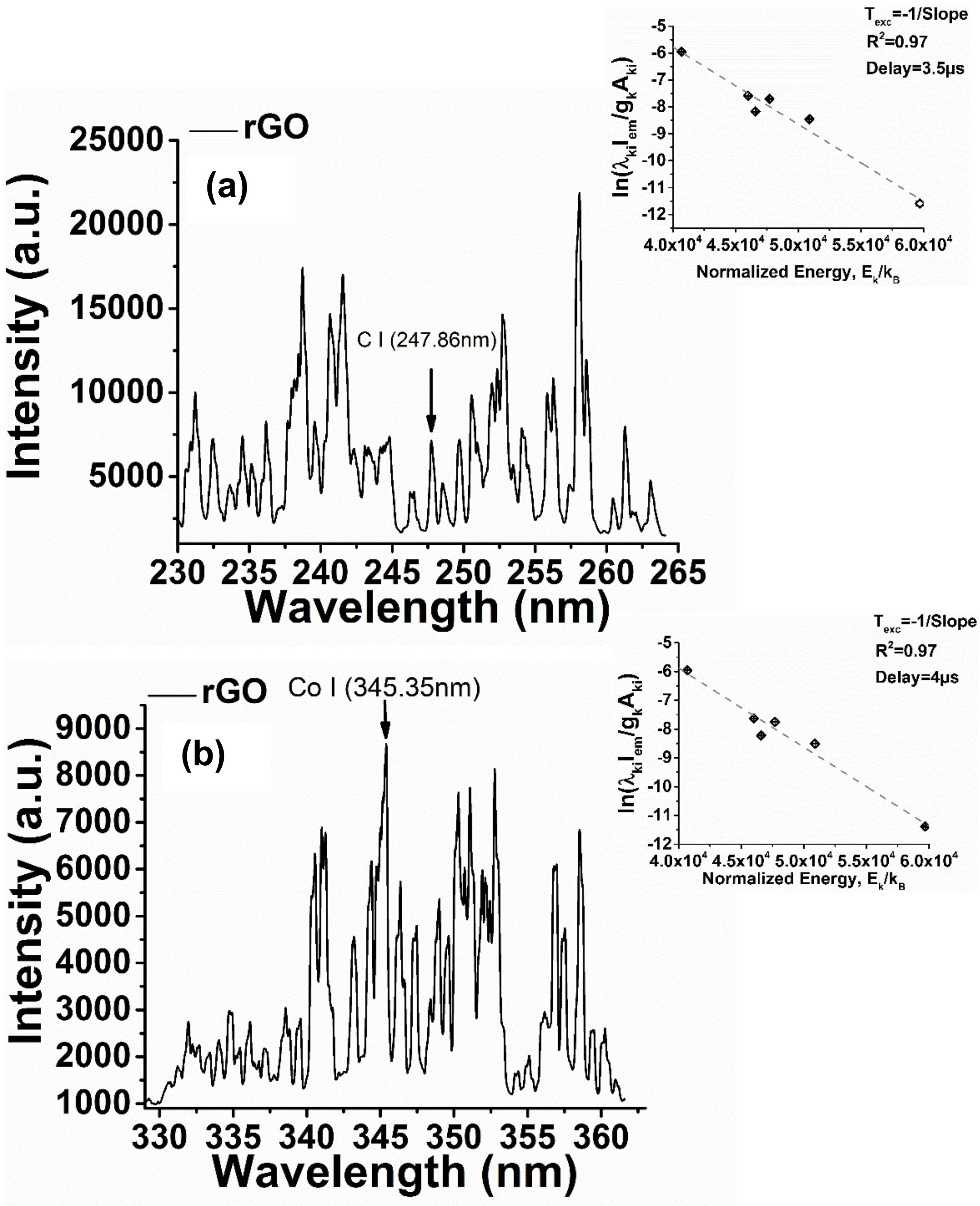

Fig. S7 Spectral emission signature for NR/rGO at (a) C I (247.86 nm), and (b) Co I (345.35 nm) lines at the respective gate delays of 3.5 μs, and 4 μs (Spectral details provided in Table S2). Inset shows the linear Boltzmann plots generated from Co I lines listed in Table S3, and used for T_{exc} calculations at the respective gate delays of 3.5 μs and 4 μs.

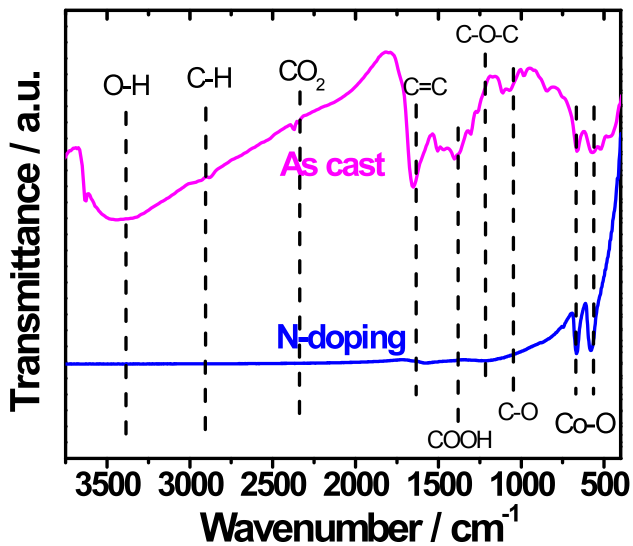

Fig. S8 FTIR results for NP/rGO (RT) and NP/NGO.

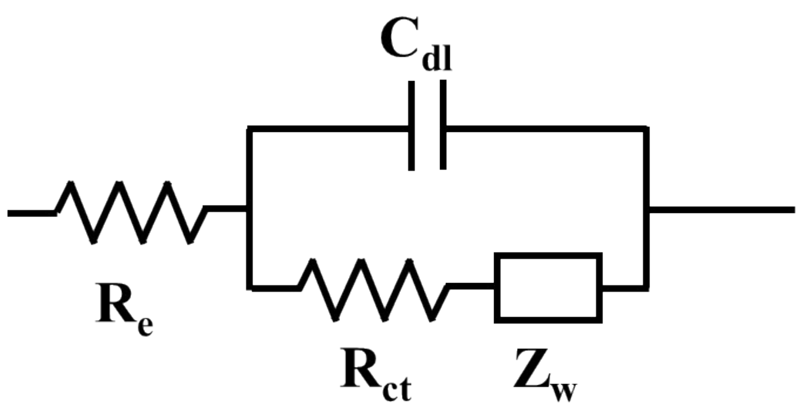

Fig. S9 equivalent circuit for the EIS results shown in Fig. 8.d.

Table S1 Comparison of the d-spacing of the as-synthesized products with standard values.

Standard Co_3O_4 d-spacing (A)	Experimental d-spacing (A)		
	NP/rGO	NR/rGO	NP/NGO
2.86 (220)	2.86	2.86	2.85
2.44 (311)	2.44	2.44	2.42
2.02 (400)	2.01	2.02	2.01
1.56 (333)	1.57	1.55	1.55
1.43 (440)	1.44	1.44	1.43

Table S2. Atomic spectral database[4] for the C I and Co I spectral emission lines shown in Fig. S6 & S7, and used for the population calculation for rGO and NGO.

Element	Wavelength (nm)	Transition probability (10^6 1/s)	Upper energy level (eV)	Lower energy level (eV)	g_k	g_i
C I	247.86	28	7.684	2.684	3	1
Co I	345.35	110	4.026	0.432	12	10

Table S3. Atomic spectral database[4] for Co atomic transition lines used for the plasma temperature calculations at 3.5μs and 4us, and internal calibration.

Element	Wavelength (nm)	Transition probability (10^6 1/s)	Upper energy level (eV)	Lower energy level (eV)	g_k	g_i
Co I	240.73	360	5.148	0	12	10
Co I	344.36	69	4.112972	0.513624	8	8
Co I	345.35	110	4.020881	0.431815	12	10
Co I	350.228	80	3.970904	0.431815	8	10
Co I	352.68	13	3.514	0	10	10
Co I	356.93	150	4.395	0.923	8	8

Reference

1. Mukherjee, D.; Rai, A.; Zachariah, M. R., Quantitative Laser-Induced Breakdown Spectroscopy for Aerosols Via Internal Calibration: Application to the Oxidative Coating of Aluminum Nanoparticles. *J Aerosol Sci* **2006**, *37*, 677-695.

2. Mukherjee, D.; Cheng, M. D., Characterization of Carbon-Containing Aerosolized Drugs Using Laser-Induced Breakdown Spectroscopy. *Appl Spectrosc* **2008**, *62*, 554-562.

3. Davari, S. A.; Hu, S.; Mukherjee, D., Calibration-Free Quantitative Analysis of Elemental Ratios in Intermetallic Nanoalloys and Nanocomposites Using Laser Induced Breakdown Spectroscopy (Libs). *Talanta* **2016**.

4. Kramida, A., Ralchenko, Yu., Reader, J. and NIST ASD Team Nist Atomic Spectra Database (Version 5.3). http://physics.nist.gov/asd